SSC20-II-05

CAT Differential Drag Implementation and Lessons Learned

Dawn Moessner and Wen-Jong Shyong
Johns Hopkins University Applied Physics Laboratory
11100 Johns Hopkins Rd, Laurel, MD 20723; 240-228-9137
dawn.moessner@jhuapl.edu

ABSTRACT

The CubeSat Signal Preprocessor Assessment and Test (CAT) spacecraft were deployed via Nanoracks from the International Space Station on January 31, 2019 and have successfully operated for over a year. These twin 3U configuration spacecraft rely on differential drag to maintain desired in-track separation distances of 10 – 150 km. The design and implementation of the differential drag maneuvers is presented along with the on-orbit results. Lessons learned throughout the past 1.5 years of spacecraft operations as well as updates to how the orbit determination and differential drag planning are conducted are also discussed. The CAT mission has been considered a success and an extended mission has been proposed to operate the spacecraft until their estimated re-entry in mid-2021.

INTRODUCTION

The CubeSat Signal Preprocessor Assessment and Test (CAT) Flight Demonstration Mission, sponsored by the US government, operates two 3U CubeSats in LEO within 150km along-track separation, each carrying an industry-provided RF instrument. Deployed from the International Space Station via Nanoracks on January 31, 2019, the spacecraft have successfully operated for 1.5 years. Each of the CAT spacecraft, built by Blue Canyon Technologies (BCT) and operated by the Johns Hopkins University Applied Physics Laboratory (JHU/APL), consists of a 3U configuration with two deployed solar panels. Lacking a propulsion system, these twin spacecraft rely on differential drag to maintain desired in-track separation.

The use of differential drag for relative formation control has become more appealing as the popularity of CubeSats and other small satellites has increased. These smaller satellites can have fairly low ballistic coefficients due to their small mass, causing atmospheric drag to have a larger effect on the trajectory. Many missions consisting of small satellites rely on having several lower-cost spacecraft platforms with smaller instrument suites in order to accomplish their mission.[1] However, the most common source of propulsion for these spacecraft are cold-gas thrusters with relatively small capability.

The concept of using deployable drag panels for formation control was introduced by Leonard et. al.[2] in the late 1980s, and research into various differential drag concepts and control algorithms has since been quite extensive.[3] Differential drag was initially utilized on orbit as a means of stationkeeping. The ORBCOMM constellation successfully used differential drag as its primary means of maintaining relative intra-plane satellite spacing.[4] As the nanosatellite class became more popular, The Aerospace Corporation launched the AeroCube-4 mission in 2012, which used deployable drag panels to successfully demonstrate deliberate formation control of a CubeSat.[5] Since 2014, Planet Labs has utilized differential drag to configure and maintain increasingly larger constellations of their dove satellites.[3,6] More recently, NASA's CYGNSS mission positioned and maintains a widely spaced constellation of 8 smallsats.[7,8] The CAT spacecraft continue to use basic differential drag control to maintain in-track separation distances between 10 and 150 km.

Throughout the past year and a half of spacecraft operations, there have been lessons learned and modifications to how the orbit determination (OD) and differential drag planning are conducted. This paper will discuss the initial implementation of differential drag for CAT. The on-orbit results and lessons learned will be discussed along with various updates to the spacecraft operations that have occurred over the past 1.5 years of CAT's successful mission.

DIFFERENTIAL DRAG

The ballistic coefficient on a spacecraft in low Earth orbit can be manipulated by increasing or decreasing the spacecraft's velocity-facing area, thus controlling the spacecraft's rate of altitude loss due to atmospheric drag. Differential drag occurs when two or more spacecraft in the same orbit have different ballistic coefficients. This creates a force differential that can be used in lieu of

propellant to control the in-track separation of two or more spacecraft. When the lead spacecraft's ballistic coefficient is decreased relative to the following spacecraft's coefficient, the leader will lose altitude at a slightly faster rate causing its velocity and the separation rate between the spacecraft to increase. If the follower's ballistic coefficient is decreased instead, then the follower will lose altitude at a slightly faster rate compared to the leader causing the rate of separation between the spacecraft to decrease.

Originally conceived as a mission without formation control, the two CAT spacecraft were not required to have propulsion. However, during development, the possibility of maintaining in-track separation distances using differential drag was examined and deemed feasible. Prior to launch, the mission chose to implement this formation control option.

Spacecraft

Each of the identical CAT spacecraft has a 3U CubeSat configuration with two deployed solar panels about 15 cm wide by 30 cm tall. A simplified drawing of the spacecraft as well as the spacecraft's body axis (x_{sc}, y_{sc}, z_{sc}) definition can be seen in Figure 1. The right solar panel faces perpendicular to the $-x_{sc}$ axis, while the second panel is canted 10° about the $-z_{sc}$ axis. Each vehicle contains a GPS unit on the $-z_{sc}$ side of the spacecraft to be used for orbit determination and onboard position, velocity, and time (PVT) knowledge. The s-band antenna for command uplink and telemetry downlink is located on the $+z_{sc}$ side of the spacecraft opposite the GPS. While in sunlight, the spacecraft is nominally pointed with solar panel surfaces to the Sun. During eclipse, attitude maneuvering for differential drag can take place without interfering with spacecraft power levels.

Drag Attitude Modes

As with the Planet Labs and CYGNSS spacecraft, the CAT spacecraft takes advantage of fixed deployed solar panels to create attitudes with varying ballistic coefficients.[3,7] True maximum or minimum drag on the spacecraft occurs when the respective maximum or minimum cross-sectional area of the spacecraft is aligned with the velocity vector relative to the atmosphere.

The CAT attitude reference frame for commanding is a local velocity local horizontal (LVLH) reference frame defined as the +*Z*-axis aligned with the nadir direction, the +*X*-axis constrained toward the inertial velocity direction, and the +*Y*-axis completing the right-handed set. The spacecraft orbit is close enough to circular that for the purposes of attitude modes, the +*X*-axis in the CAT LVLH frame can be assumed to point to the inertial velocity. For daily commanding simplicity, the LVLH +*X*-axis (i.e. the inertial velocity vector) is used instead of the atmospheric-relative velocity vector as a reference for the drag attitude modes. However, when attitude and drag are modeled in Orbit Determination Tool Kit (ODTK) or Systems Tool Kit (STK), the velocity relative to an Earth-centered Earth-fixed (ECEF) frame is used to approximate the atmospheric-relative velocity.

Table 1 lists the attitude definition as well as the resulting cross-sectional area for each of the mission's drag attitude modes. CAT achieves a maximum to minimum

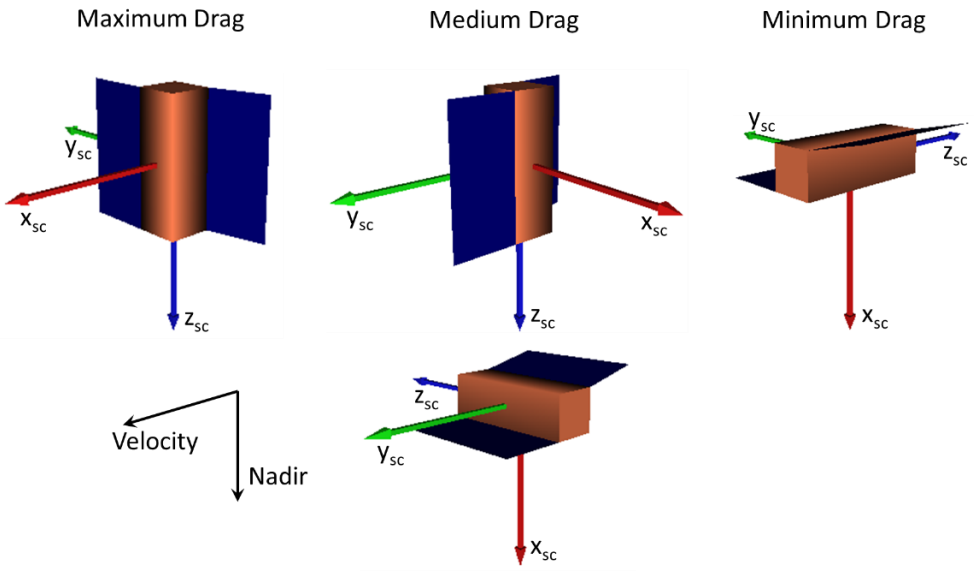

Figure 1: CAT attitudes utilized to achieve varying amounts of atmospheric drag.

drag area ratio of 12:1 and a maximum to medium drag area ratio of 3:1. Each of these attitude modes is also depicted in Figure 1 using a simplified drawing of the spacecraft. Furthermore, each of these orientations ensures that the Earth keep-out zone remains clear for at least one of the spacecraft's two star trackers.

Table 1: CAT drag attitude modes and cross-sectional areas.

Attitude Mode	Spacecraft Axis Toward Velocity	Spacecraft Axis Aligned with Nadir	Cross-Sectional Area (m^2)
Maximum Drag	$+x_{sc}$	$+z_{sc}$	0.121
Medium Drag (GPS to Zenith)	$+y_{sc}$	$+z_{sc}$	0.041
Medium Drag (GPS to Port)	$+y_{sc}$	$+x_{sc}$	0.041
Minimum Drag	$-z_{sc}$	$+x_{sc}$	0.010

MODELING

ODTK and STK/Astrogator were selected for performing spacecraft OD, predicted trajectory propagation, and differential drag maneuver targeting. The spacecraft telemetry included filtered GPS PVT data from which the position and time information were converted to a NAVSOL format for input to the Kalman filter in ODTK. The drag coefficient, Cd, for the spacecraft was to be estimated through the OD process. For both ODTK and STK, plugins were developed to calculate the drag cross-sectional area based on spacecraft attitude using a flat-plate model of the spacecraft.

Calculation of Drag Cross-Sectional Area

To compute the drag force, the cross-sectional area in the plane normal to the ECEF velocity direction needed to be computed. Given the plate model of the CAT spacecraft, this area is calculated for each plate in which the angle between the plate normal and the ECEF velocity direction is <90°. Due to the presence of deployed solar panels on the CAT spacecraft, one plate may overlap another plate, thus causing a certain area of the back plate to be blocked as in Figure 2. The shaded, convex polygon in the figure represents the area of the back plate blocked by the front plate when viewed from opposite the ECEF velocity direction. The projected area, A_P, of each plate into the plane normal to the ECEF velocity direction is calculated. If that plate is overlapped by another, the overlapping area, A_O, is then calculated.

To calculate A_O, a local coordinate system is first defined by using one corner point of the back plate as the origin. The *x*-axis is a vector along the edge of two adjacent corner points of the back plate and the *z*-axis is perpendicular to the back plate. The *y*-axis is then the cross product of the *z*-axis to *x*-axis. All points of the front and back plates are converted from the original body-fixed frame to this local coordinate system. Then the front plate is projected along the ECEF velocity direction to the plane of the back plate as shown in Figure 2. The edges surrounding area A_O will be connected by three or more bounding points. These bounding points are either corner points of a plate within another plate, or intersection points of overlapping plate edges and/or corners. For this example, there are four bounding points. Point 2 is a corner point of the front plate within the back plate, and point 4 is the corner point of the back plate within the front plate. Points 1 and 3 are intersection points of two overlapping plate edges.

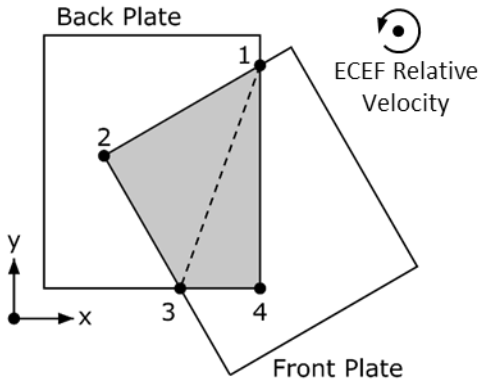

Figure 2: Plates projected into the plane normal to the ECEF velocity vector. When calculating drag cross-sectional area, one plate may block another.

In the CAT spacecraft plate model, all plates are rectangles, that is, they are all convex polygons. The overlapping area of two convex polygons is also a convex polygon. Once the bounding points $(P_1, P_2, \dots, P_n)$ are determined, the centroid point, *C*, of $(P_1, P_2, \dots, P_n)$ is found. Since the overlapping area is a convex polygon, *C* is within the overlapping area. We define the set of vectors $(\overline{CP_1}, \overline{CP_2}, \dots, \overline{CP_n})$ from *C* to each bounding point. All of these vectors will be entirely contained within the overlapping area. Next, the bounding points are sorted in order of increasing angle between the *x*-axis and the vector $\overline{CP_n}$. We relabel these points as $(S_1, S_2, \dots, S_n)$ according to this order. The polygon is now divided into multiple triangles of (S_1, S_2, S_3), (S_1, S_3, S_4), …, (S_1, S_{n-1}, S_n). The area A_O is then the sum of the triangular areas. The drag cross-sectional area, A_C, of the back plate is then, $A_C = A_P - A_O$. For plates that are not overlapped, A_C is simply equal to A_P. The drag cross-sectional area for the spacecraft is then $\sum(A_{C1} + A_{C2} + \dots + A_{Cn})$, where *n* is the number

of spacecraft plates for which the angle between the plate normal and the ECEF velocity direction is <90°.

Drag Maneuver Planning

Differential drag maneuvers would be needed in two phases. After initial deployment the spacecraft will be separating with CAT-1 ahead of CAT-2. The first phase would counteract the acceleration from deployment and bring the spacecraft back below 150 km separation if necessary. Based on deployment velocity specifications provided by Nanoracks and spring force models of the spacecraft separation mechanism, it was estimated that counteracting the initial deployment acceleration could take several days and that the spacecraft were unlikely to exceed the 150 km separation limit.

Once the initial deployment acceleration was halted, the drag maneuver planning would enter a formation maintenance phase. Initially, drag maneuvers were planned and updated on a weekly basis. The separation of the two CAT spacecraft was to be maintained between 10 km and 150 km with CAT-1 always remaining ahead of CAT-2. The mission design and navigation (MD/NAV) team selected a target separation distance of 75±25 km and a 0±1 km/day target separation rate. Each week, the initial state would be propagated forward 5 weeks in STK and if either the separation distance or the separation rate exceeded the set bounds, drag maneuvers would be added. The first set of maneuvers would bring the spacecraft back to the target separation over the next 1-2 weeks and a second set of maneuvers would halt the separation rate once the target separation was achieved. The mission operations team (MOT) would input these maneuver times and attitude quaternions to CATApp, the CAT mission's command planning tool. CATApp is built on SciBox, a space operational planning and commanding technology.[9] When run, CATApp coordinates and updates all spacecraft commanding including contacts, payload operations, and drag maneuvers, then outputs the daily command sequences to be uploaded to the spacecraft.

ON-ORBIT: RESULTS AND LESSONS LEARNED

Not unlike other satellites of this class, CAT has encountered and had to work around safe-mode demotions and operational issues that are fairly common with this class of satellite.[6,8] The CAT team has been responsive in creating solutions that have allowed the mission to continue successfully.

Deployment

The spacecraft were deployed into orbit via Nanoracks on January 31st, 2019, 10:25 UTC and CAT-1 began moving ahead relative to CAT-2. The solar panels successfully deployed on both spacecraft and each spacecraft's beacon was detected during the first contact with the JHU/APL satellite communications facility (SCF) at 18:34 UTC. As spacecraft check-out continued over the next several contacts, it was apparent that neither spacecraft's GPS was able to track enough satellites for a valid solution. Because of this, JSPOC TLEs were used for orbit determination and prediction over the next several days.

Initially, the nominal attitude during eclipse was a minimum drag orientation to prolong lifetime; however, 6 days after deployment, the nominal eclipse attitude was changed to have the GPS pointed to zenith to aid the spacecraft in acquiring GPS satellites. This solution was successful on CAT-2, but not on CAT-1. Once GPS data was available for CAT-2, it was ingested into ODTK to produce a definitive ephemeris as originally planned, while CAT-1 continued to utilize TLEs. Ultimately, the CAT-2 GPS would also stop acquiring satellites in July 2019 and TLEs would be used for both satellites from that point forward.

To counteract the separation acceleration from deployment, it was desired to place CAT-2 in maximum drag mode while CAT-1 remained in a medium drag mode with GPS to zenith. However, there was an error in the attitude commanding that took several days to diagnose. As a result, the CAT-2 spacecraft did not actually enter maximum drag attitude until February 13th. The spacecraft separation during the initial 6 weeks after deployment can be seen in Figure 3, where the blue line is the spacecraft separation according to TLE data and the orange box represents the required separation range. Several discontinuities appear in the separation distance data between Feb 1st and Feb 6th due to an absence of TLE data during this time.

Because the spacecraft were set to exceed the desired separation distance shortly after CAT-2 achieved maximum drag attitude, CAT-1 was changed to a minimum drag mode during eclipses to maximize the drag differential. Since the spacecraft GPS on CAT-1 had still not provided a valid solution, halting the spacecraft separation quickly was deemed a higher priority than keeping the CAT-1 GPS pointed to zenith. It can be seen in the plot that the spacecraft responded well and within 10 days went from an 11.6 km/day separation rate to a 0 km/day separation rate. This equaled an average -1.16 km/day^2 acceleration due to differential drag. On March 4th the spacecraft separation came within 150 km and the drag maneuver planning became focused on formation maintenance.

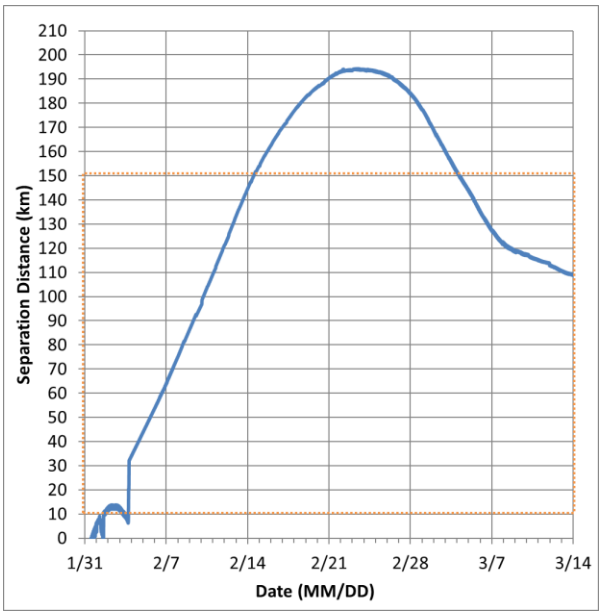

Figure 3: CAT spacecraft separation distance during the first 6 weeks post deployment

Formation Maintenance

Once the spacecraft had achieved a sufficient closing rate, drag maneuvers were halted, and both spacecraft were commanded to resume the medium-drag mode with GPS to zenith during eclipses. Meanwhile, the remainder of the spacecraft check-out and payload commissioning was continuing and completed successfully on March 17th. On March 21st the payload began primary operations. Figure 4, below, contains the spacecraft separation distance from launch through June 2020. During the initial months on-orbit, it became apparent that several challenges, including the lack of GPS data for one spacecraft and frequent safe-mode demotions or command lock-outs, meant MD/NAV would need to modify some aspects of the differential drag planning. The percentage of time between February 8th, 2019, and May 16th, 2020, that each spacecraft has spent in maximum drag maneuvering or safe-mode is shown in Table 2. Both spacecraft have spent a similar percentage of time in safe-mode; however, CAT-1 has required more maximum drag maneuvers than CAT-2, indicating a possible overall closing trend between the two spacecraft.

Table 2: Percentage of time each spacecraft has spent in maximum drag maneuvering or safe-mode

Spacecraft	% of Orbits with Maximum Drag Maneuvers	% of Time On-Orbit in Safe Mode
CAT-1	15.6	14.1
CAT-2	11.2	14.4

A safe-mode demotion or command lock-out during the week could unfavorably change the spacecraft separation rate quickly enough that weekly corrections were not always sufficient. Furthermore, if a demotion occurred when drag maneuvering was scheduled, waiting a week to reschedule maneuvers was not desirable. To handle these instances, MD/NAV and the MOT worked together to implement a process to manually add drag maneuver commands to a command load. These drag attitude commands would occur in

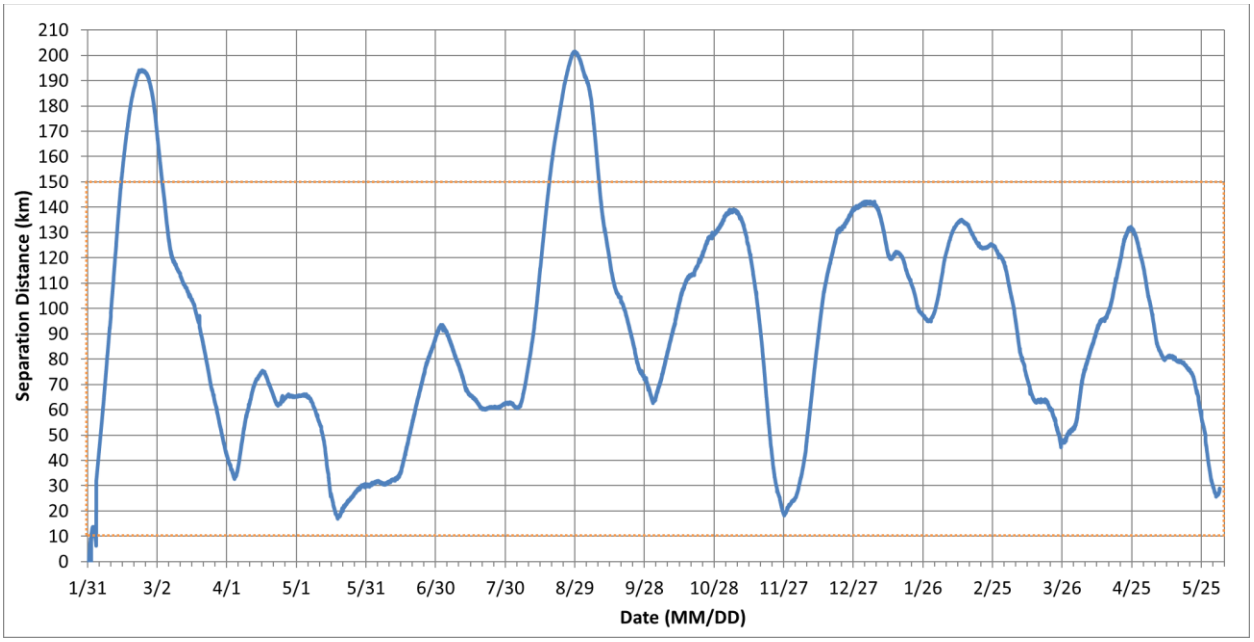

Figure 4: Spacecraft separation distance from launch on January 31, 2019 through June 2, 2020

addition to any drag attitude commands added through the CATApp command load generation process.

One of the first instances where manual commanding was needed coincides with the first dip in spacecraft separation seen in late March and early April of 2019 in Figure 4. Within a week various demotions to safe mode had caused the spacecraft closing rate to increase. When maximum drag maneuvers were scheduled on CAT-1, further safe mode demotions prevented them from executing. Ultimately, CAT-2 was manually placed in a minimum drag mode whenever it was out of safe mode and CAT-1 was able to perform 2 days of manually added maximum drag maneuvers.

Situations similar to this continued to occur about once every 1-2 months. One of the more notable events occurred in August when untimely safe-modes and command lock-outs prevented maximum drag maneuvers scheduled through the weekly process from executing on CAT-2. When manual commands were finally able to be executed, 5 days of drag maneuvers were required and the spacecraft reached a maximum 201-km separation. If manual maneuvers had been added more aggressively in early August when the separation trend was first noted, the spacecraft likely would not have exceeded the 150-km separation limit. Therefore, the MD/NAV team began checking the spacecraft separation using mid-week TLE data and requesting manual maneuvers if the spacecraft seemed to be suddenly deviating from their previous separation rates. MD/NAV also raised the target separation distance to 95±25 km in early December 2019 after the spacecraft came within < 20 km for the second time.

Cd Estimation

Originally planned to be estimated through the OD process, the use of TLE data presented a challenge for estimating spacecraft Cd. During the first several months of operation, the Cd for each spacecraft was estimated each week based on a fit to the previous two weeks of ephemeris. For CAT-1 this continued to be the TLE data. For CAT-2 this was the definitive ephemeris from ODTK for the time that it was available and later the TLE data. After some trial and error, it was found that using the average of these two Cd values for both spacecraft was more successful than using the individual values. Figure 5 displays the weekly estimated Cd for each spacecraft through early October 8th, 2019. At that time, it had become evident that the Cd fit was being affected by unpredictable safe-mode attitudes and other effects that weren't included in the ephemeris modeling. Although the past Cd fit did not seem to be a good predictor of future Cd values, it did remain bounded. Therefore, an average Cd value of 1.32 was calculated and utilized on both spacecraft going forward.

Updated Drag Maneuver Process

In February 2020, MD/NAV began testing an updated process for calculating the required differential drag maneuvers. It was desired to make the drag maneuver design and commanding more frequent and responsive. To accomplish this, the latest TLE for each spacecraft is propagated forward and the current separation, s, and separation rate, $\dot{s}$, are calculated. The desired spacecraft separation is $s_d = 95$ km ±5 km. The desired separation rate for $s \leq 90$ km or $s > 100$ km is $\dot{s_d} = (s_d - s)/t$ and for 90 km $< s \leq 100$ km is $\dot{s_d} = 5/t$, where $t = 21$ days. The small separation rate when at the desired separation is to counteract the overall slight closing trend that the spacecraft have exhibited. Bounds are placed on $\dot{s_d}$ that become incrementally tighter as the separation is closer to 95 km. If $\dot{s}$ exceeds the set bounds on $\dot{s_d}$, then maximum drag maneuvers are needed and the required change in separation rate is then calculated.

If the required change in separation rate, $\Delta\dot{s} = \dot{s_d} - \dot{s}$, is positive, then the maneuvers will be executed on CAT-

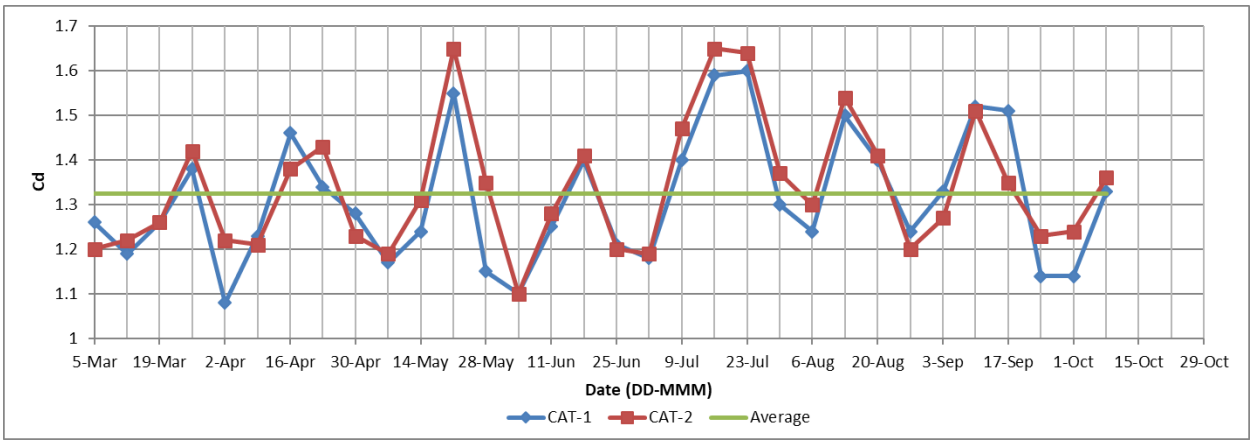

Figure 5: Weekly estimated and overall average Cd values for the CAT spacecraft

1, if $\Delta\dot{s}$ is negative, then the maneuvers will be executed on CAT-2. The total duration of drag maneuvering required to accomplish $\Delta\dot{s}$ is calculated based on previous results and modeling of the effectiveness of the differential drag maneuvers. Given the current length of eclipses, the total duration is divided into the number of eclipses for which maximum drag maneuvers are then manually added to the appropriate spacecraft's next available command load. The drag maneuver calculation is currently performed twice a week with at least three days between updates. This allows a day for the command load to be uploaded, one day for the command execution, and one day for the TLE to reflect changes in the trajectory.

Even with this new process being performed, in part, manually, the time required to plan and implement the drag maneuver commands has decreased from close to 8 hours/week to < 2 hours/week. Ultimately, MD/NAV plans to work with the CATApp team to incorporate these drag maneuver calculations into the CATApp automation. This would result in more effective scheduling of the drag maneuvers and eliminate the need for regular manual modifications to the command loads.

CONCLUSION

The CAT mission has successfully utilized differential drag to maintain the in-track separation of its twin spacecraft. Despite the challenges presented involving the GPS and spacecraft demotions, the CAT spacecraft have only exceeded the desired separation range twice in the past 1.5 years of operations. The first excursion was due to a combination of initial deployment velocity and delayed initiation of differential drag attitude maneuvering. The second was due to untimely safe-mode demotions and command lock-outs. During the past 4 months of operations, more frequent drag maneuver updates were implemented in combination with a faster method of calculating required maneuver duration leading to more responsive control over the spacecraft separation. The primary CAT mission has been considered a success and an extended mission has been proposed that would continue to operate the twin spacecraft until their expected de-orbit in the summer of 2021.

ACKNOWLEDGEMENTS

The CAT mission was designed and operated by the Johns Hopkins University Applied Physics Laboratory under U.S. government contract. The authors would like to acknowledge additional members of the CAT MD/NAV and Mission Operations teams including Brent Duffy, Ryan Bull, Brian Lathrop, Ryan Mitch, and Paul Boie for their previous and ongoing contributions to CAT differential drag operations.

REFERENCES

1. Chung, S.J., S. Bandyopadhyay, R. Foust, G.P. Subramanian, F.Y. Hadaegh, "Review of Formation Flying and Constellation Missions Using Nanosatellites," Journal of Spacecraft and Rockets, vol. 53, no. 3, pp. 567-578, May-June 2016.
doi: 10.2514/1.A33291

2. Leonard, C.L., W.M. Hollister, and E.V. Bergman, "Orbital Formationkeeping with Differential Drag," Journal of Guidance, Control, and Dynamics, vol. 12, no. 1, pp. 108-113, 1989.

3. Foster, C., J. Mason, V. Vittaldev, L. Leung, V. Beukelaers, L. stepan, and R. Zimmerman, "Constellation Phasing with Differential Drag on Planet Labs Satellites," Journal of Spacecraft and Rockets, vol. 55, no. 2, pp. 473-483, March-April 2018.
doi: 10.2514/1.A33927

4. Maclay, T.D. and C. Tuttle, "Satellite Stationkeeping of the ORBCOMM Constellation via Active Control of Atmospheric Drag: Operations, Constraints, Performance (AAS 05-152)," Advances in the Astronautical Sciences, vol. 120, 2005.

5. Gangestad, J.W., B. S. Hardy, and D. A. Hinkley, "Operations, Orbit Determination, and Formation Control of the AeroCube-4 CubeSats (SSC13-X-4)," Proceedings of the 27th Annual AIAA/USU Conference on Small Satellites, Logan, UT, Aug. 2013.

6. Foster, C., H. Hallam, and J. Mason, "Orbit Determination and Differential-Drag Control of Planet Labs CubeSat Constellations (AAS 15-524)," Proceedings of the AAS/AIAA Astrodynamics Specialist Conference, Vale, CO, Aug. 2015.

7. Finley, T., D. Rose, K. Nave, W. Wells, J. Redfern, R. Rose, and C. Ruff, "Techniques for LEO Constellation Deployment and Phasing Utilizing Differential Aerodynamic Drag (AAS 13-797)," Advances in the Astronautical Sciences, vol. 150, pp. 1397-1411, 2013.

8. Bussy-Virat, C.D., A.J. Ridley, A. Masher, K. Nave, and M. Intelisano, "Assessment of the Differential Drag Maneuver Operations on the CYGNSS Constellation," IEEE Journal of Selected Topics in Applied Earth Observations and Remote Sensing, vol. 12, no. 1, pp. 7-15, Jan. 2019.
doi: 10.1109/JSTARS.2018.2878158

9. Choo, T.H., A.F. Berman, H. Nair, L. Nquyen, J.P. Skura, and R.J. Steele, “SciBox: An Autonomous Constellation Management System,” Johns Hopkins APL Technical Digest, vol. 33, no. 4, pp. 314-322, 2017. https://www.jhuapl.edu/Content/techdigest/pdf/V33-N04/33-04-Choo.pdf